Int. J. Electrochem. Sci., 7 **(2012)** 4988 - 4999

International Journal of
ELECTROCHEMICAL
SCIENCE
www.electrochemsci.org

Photoelectrode Optimization of Zinc Oxide Nanoparticle Based Dye-Sensitized Solar Cell by Thermal Treatment

Pichanan Teesetsopon[1], *S. Kumar*[1] *and Joydeep Dutta*[2,3,*]

[1] Energy Field of Study, Asian Institute of Technology, Klong Luang, Pathumthani 12120. Thailand
[2] Center of Excellence in Nanotechnology, Asian Institute of Technology, Klong Luang, Pathumthani 12120. Thailand
[3] Chair in Nanotechnology, Water Research Center, Sultan Qaboos University, PO Box 17, Postal Code 123, Al Khoud, Oman
[*]E-mail: joy@ait.asia; dutta@squ.edu.om

Received: 18 April 2012 / *Accepted:* 21 April 2012 / *Published:* 1 June 2012

Interfacial properties at the photoelectrode of dye-sensitized solar cell (DSSC) play a vital role in determining its efficiency. This research examined the role of annealing temperature on the photoelectrode interfaces properties, and to find the annealing temperature that provides the highest overall solar cell efficiency. The electrical characteristics of the DSSC using ZnO nanoparticles photoelectrode annealed at different temperatures were studied using electrochemical impedance spectroscopy (EIS), and the corresponding I-V characteristics were determined. The highest efficiency of the solar cells was obtained when the photoelectrode was annealed at 400°C. This is mainly due to the enhancement in charge collection by better ZnO crystallinity and reduction of interfacial charge transfer resistance at the ZnO/dye/electrolyte interface. Moreover, the electron recombination between transparent conducting oxide substrate and electrolyte was also revealed for the first time by EIS.

Keywords: ZnO, Photoelectrode; Dye-sensitized solar cell; Annealing; Electrochemical impedance spectroscopy; Interface resistance; Recombination

1. INTRODUCTION

Dye-sensitized solar cells (DSSC) offer the possibility of reducing the cost of photovoltaic (PV) technology at reasonable efficiency, and thus expand the reach of solar energy for practical applications [1]. A number of attempts have been made for developing dye-sensitized solar cell (DSSC) in the past decade [2-5]. The light harvesting idea of DSSC mimics photosynthesis in nature in the sense that dye molecules can absorb sunlight and convert it into a required form of energy (chemical energy for plant and electrical energy for DSSC) [3]**.** Unlike silicon based solar cells, the

semiconductors used in DSSC are readily synthesized and available at reasonable costs. Semiconducting materials play the role of charge transfer medium in the case of DSSC. In DSSC, the light harvesting material and the charge transfer medium are separated, slightly lower material quality is acceptable, and this helps lower manufacturing costs. Energy conversion efficiency, as high as 11.1%, have been reported for DSSC based on wide band gap semiconductor titanium dioxide (TiO_2) nanoparticles [6].

DSSC is a capacitive device, composed of a wide band gap nanostructured semiconductor coated on a transparent conducting oxide (TCO) photoelectrode, organic dye molecules for light harvesting, electrolyte (normally I_3^-/I^- in acetronitrile) as a supplier of charges and a catalyst (usually platinum) to activate the charges in the electrolyte that is deposited on the counter electrode. The interfacial properties between each component play a crucial role in DSSC efficiency. The main reason for using a nanostructured material is to provide high surface area for dye adsorption to maximize light harvesting. Zinc Oxide (ZnO) is an interesting alternative wide band gap material as it has a similar band gap as TiO_2 and can be easily synthesized in various nano-structures [7]. This gives more flexibility to construct different DSSC solar cells for further improvement of efficiency and long term stability of these cells [8].

Current-voltage (*J-V*) characteristics under light illumination is used to determine the electrical properties of DSSC [9, 10], namely, cell efficiency (η), fill factor (*FF*), open circuit voltage (V_{oc}) and short circuit current density (J_{sc}). Recent studies conducted to improve the efficiency of DSSC have reported that thermal treatment can enhance the efficiency by increasing crystallinity of synthesized ZnO nanoparticles [11-13], improving adhesion between the FTO and ZnO film [14], enhancing ZnO band-gap [15], removing impurities [16], increasing pore size and surface area [17] and lowering the effects of both bulk traps and surface states [13, 18]. Improvements in the cell performances has been reported to be due to the suppression of the recombination and the decrease in the resistances existing in the cell [19]. However, no detailed study on interface resistance has yet been reported to better reflect on the understanding of the changes in electrical characteristics of these devices upon annealing the photoelectrodes of DSSC.

In this work, we have systematically studied the internal interface resistance of ZnO nanoparticles based DSSC devices using electrochemical impedance analysis and have also conducted conventional I-V characteristic investigations to explain the efficiency enhancement of DSSC due to annealing. Furthermore, we also tried to identify the complex recombination behavior occurring at the photoelectrode interface.

2. EXPERIMENTAL STUDY

ZnO nanaparticle paste was prepared by dispersing ZnO nanoparticles (Aldrich Chemical, US) in ethanol in 1:1 ratio by weight and was kept stirred for 1 hour for proper mixing. ZnO film was screen printed on fluorine doped tin oxide (SnO_2: F) coated conducting glass substrates (FTO, 12Ω/□ from Nippon Sheet Glass, Japan) followed by annealing in air at 350°C, 400°C and 450°C for 30 minutes respectively.

These photoelectrodes were then immersed in ethanol solution of 0.5 mM N719 dye [cis-dithiocyanate-N,N-bis-(4-carboxylate-4-tetrabutylamonium-carboxylate-2,2-ipyridine) ruthenium(II)] obtained from Solaronix, Switzerland for 24 hours at room temperature. Following the dye absorption, photoelectrodes were thoroughly rinsed with ethanol and stored in a dessicator under dark conditions at room temperature. The counter electrode was prepared by platinizing pre-drilled FTO with 5 µl 5 mM hydrogen hexachloroplatinate (IV) hydrate (H_2PtCl_6) solution (Fluka) by smearing on FTO substrates followed by heat treatment at 385°C for 30 minutess in air. The photoelectrode and counter elctrode were assembled using parafilm as a thermal adhesive film with an active area of **0.25** cm^2**.** The iodide/tri-iodide electrolyte prepared from a mixture of 0.5 M LiI, 0.05 M I_2 and 0.5 M 4-tertbutylpyridine (TBP, Fluka) in acetonitrile was then filled in the gap of assembled cell through one of the pre-drilled holes, taking care that no bubbles were formed, which were finally sealed with an adhesive film. Three samples for each condition were used to examine the results.

The morphologies of ZnO film under different annealing conditions were examined by field emission scanning electron microscope (FESEM). Images were taken by JEOL JSM-6301 FESEM operating at 20 kV.

The adsorption of dye was examined via optical absorption spectra obtained by using Ocean Optics USB 4000 Spectrometer. The electrical properties of DSSC cell were measured by using a programble electrometer (Keithley 617 Electrometer) under AM 1.5G illumination (1000 W/m^2) from a solar simulator (Sciencetech 150W Small Beam Solar Simulator, Model SF150). Sheet resistances of FTO under various annealing temperatures were measured via Four-Point-Probe technique. The amount of dye adsorption on ZnO NP photoelectrode was determined by de-adsorption in 0.1 mM KOH and measured with UV-VIS (Ocean Optics). The internal interface resistance and electron lifetime were extracted from electrochemical impedance spectroscopy (EIS) using Gamry Instruments model PCI4-300 Potentiostat/Galvanostat/ZRA. The frequency ranges used for the EIS measurement ranged from 100 mHz to 100 kHz with an AC modulation signal of 10 mV. EIS characterization of DSSCs was carried out under 100 mW/cm^2 illumination using PEC model L11 solar simulator under ambient temperature, and the EIS spectra were analyzed using the software Echem Analyst from Gamry Instruments Inc.

3. RESULTS AND DISCUSSION

It is well known that annealing removes impurities and consequently enhances the purity of ZnO nanoparticles without influencing its Wurtzite phase [16]. The dangling bonds mainly present at the grain boundaries reduces with the grain growth [20]. The morphologies of the ZnO nanoparticle coating on FTO photoelectrode are shown in Figure 1.

With increasing annealing temperatures, grain growth occurs resulting in higher porosity in the films (see supplementary information, Figure S1 and Table S1). We observed that sintering of ZnO nanoparticles occur as annealing temperature was increased from 350°C to 450°C. This is due to the mass transport between connecting particles [21, 22].

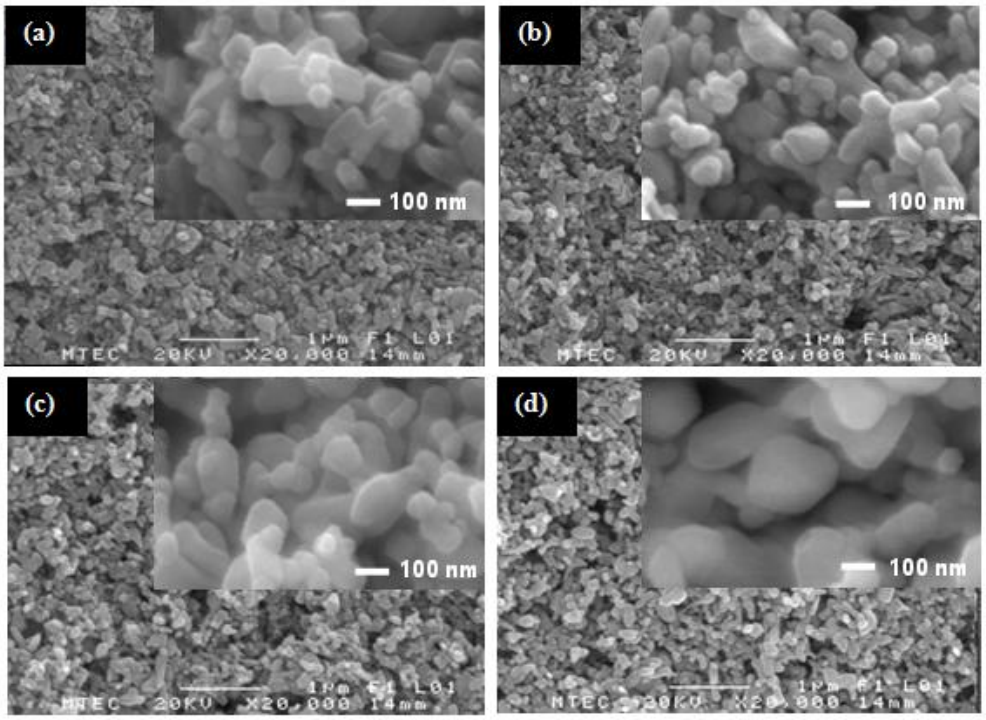

Figure 1. FESEM images show porous structure and grain size of ZnO nanoparticles annealed at different temperatures (a) 25°C, (b) 350°C, (c) 400°C and (d) 450°C

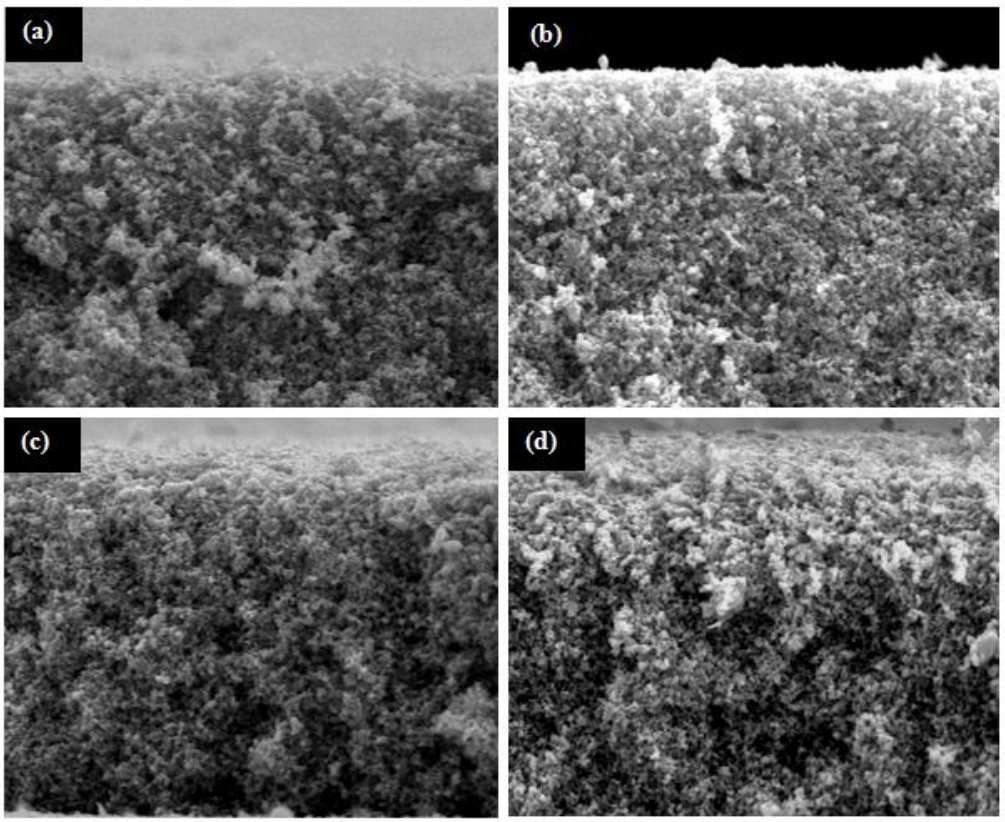

Figure S1. Cross section FESEM images show porosity of ZnO nanoparticle film annealed at different temperature (a) 25°C, (b) 350°C, (c) 400°C and (d) 450°C.

Table S1. Average grain size measured from FESEM images by ImageJ software.

Annealing temperature	Average grain size (nm)
25°C	91.2 ± 37.6
350°C	92.8 ± 34.2
400°C	119.0 ± 47.4
450°C	163.1 ± 71.5

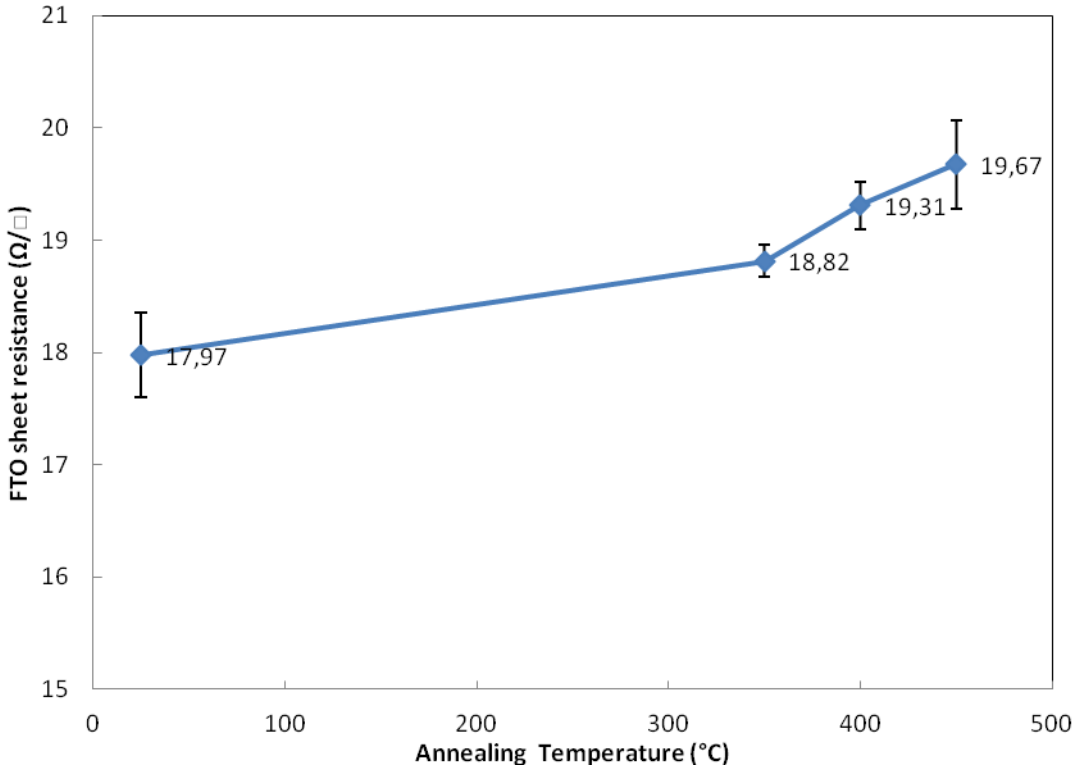

Figure S2. FTO sheet resistance variation after annealed at different temperature measured by four-point-probe technique.

The improved crystallinity and reduced grain boundary regions affect the solar cell efficiency in opposite ways. The surface area of the semiconductor reduces with increased grain growth leading to lower dye adsorption in DSSC's resulting in lower charge generation efficiency, while reduction of dangling bonds due to reduced grain boundaries improves charge collection efficiency. Hence, optimization of the grain growth and the reduction of dangling bonds are required to improve DSSC efficiencies.

The de-adsorption of dyes from different photoelectrodes annealed at varying temperatures (Figure 2) confirms the lowering of dye adsorption in samples annealed at higher temperatures. This is due to the decreasing surface area of the ZnO nanoparticles. Lower dye adsorption would lead to a reduction in light harvesting efficiency and hence the short circuit current (J_{sc}) of DSSC's should reduce upon annealing the photoelectrodes in air.

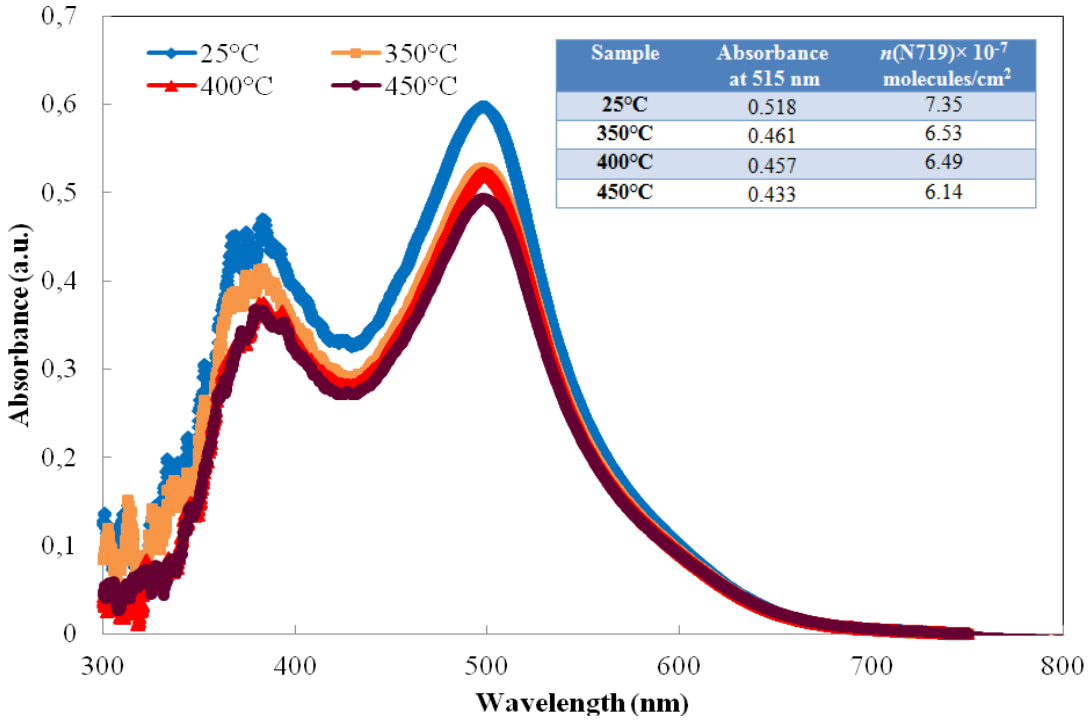

Sample	Absorbance at 515 nm	n(N719)× 10^{-7} molecules/cm^2
25°C	0.518	7.35
350°C	0.461	6.53
400°C	0.457	6.49
450°C	0.433	6.14

Figure 2. UV-VIS absorbance of dye de-adsorption from ZnO photoelectrodes at different annealing temperatures and corresponding dye adsorbed amount (enclosed Table)

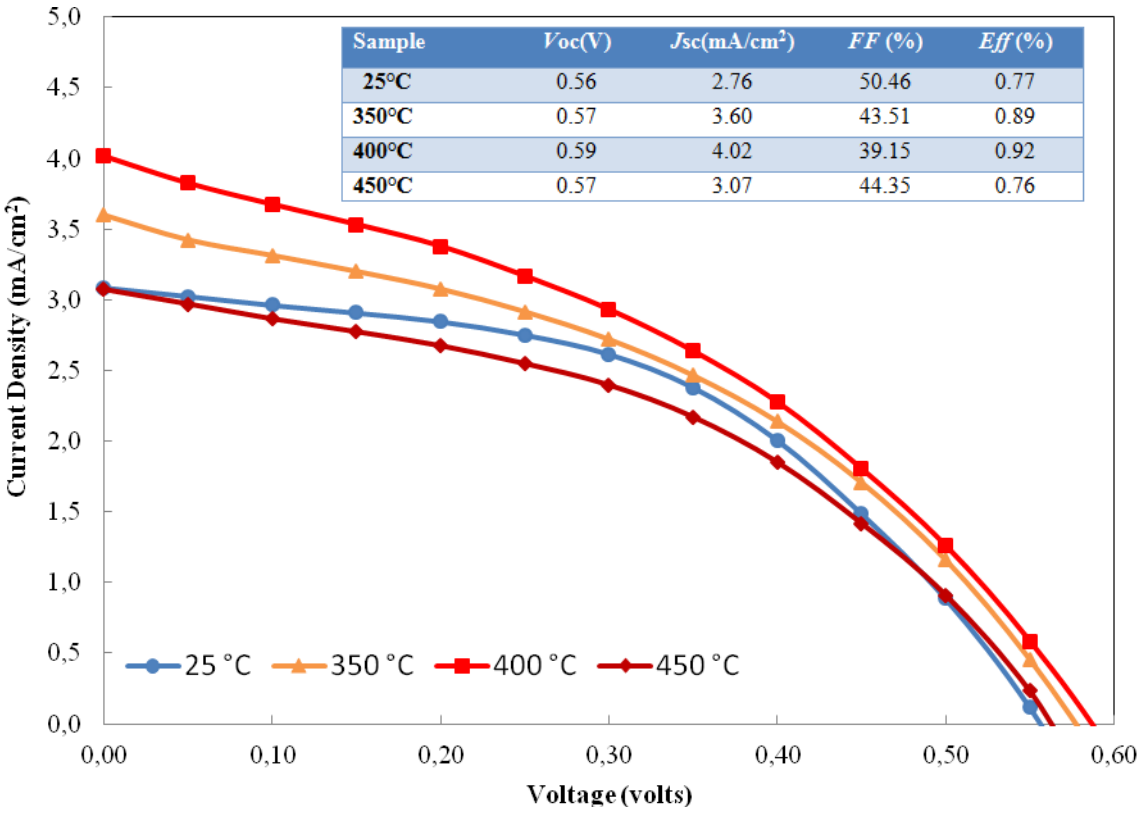

Sample	*Voc*(V)	*Jsc*(mA/cm^2)	*FF* (%)	*Eff* (%)
25°C	0.56	2.76	50.46	0.77
350°C	0.57	3.60	43.51	0.89
400°C	0.59	4.02	39.15	0.92
450°C	0.57	3.07	44.35	0.76

Figure 3. Current-Voltage characteristics of ZnO-DSSCs using ZnO nanoparticles photoelectrode annealed at different temperature.

However, it was observed that that J_{sc} increases upon annealing the photoelectrodes up to 400°C, and then decreases with further increase in the annealing temperature (Figure 3) consistent with the work reported by Lu et al. [13]. This means that more charge is obtained even though slightly lower charge generation would occur. The obtained higher current density is thus attributed to a better charge collection caused by the lowering of charge scattering at the grain boundary interfaces of the ZnO nanoparticles.

Since the conducting property of semiconductor especially the transparent conducting oxide depends strongly on defects and impurity scattering [23, 24], therefore, it is possible that, during annealing, the thermal energy is used to achieve higher mass transport between FTO substrate and ZnO layer that stimulates oxygen atoms diffusing into both the layers, resulting in a higher sheet resistance of FTO. The increase of FTO sheet resistance (R_{FTO}) upon annealing was confirmed by four-point-probe method (see supplementary formation, Figure S).

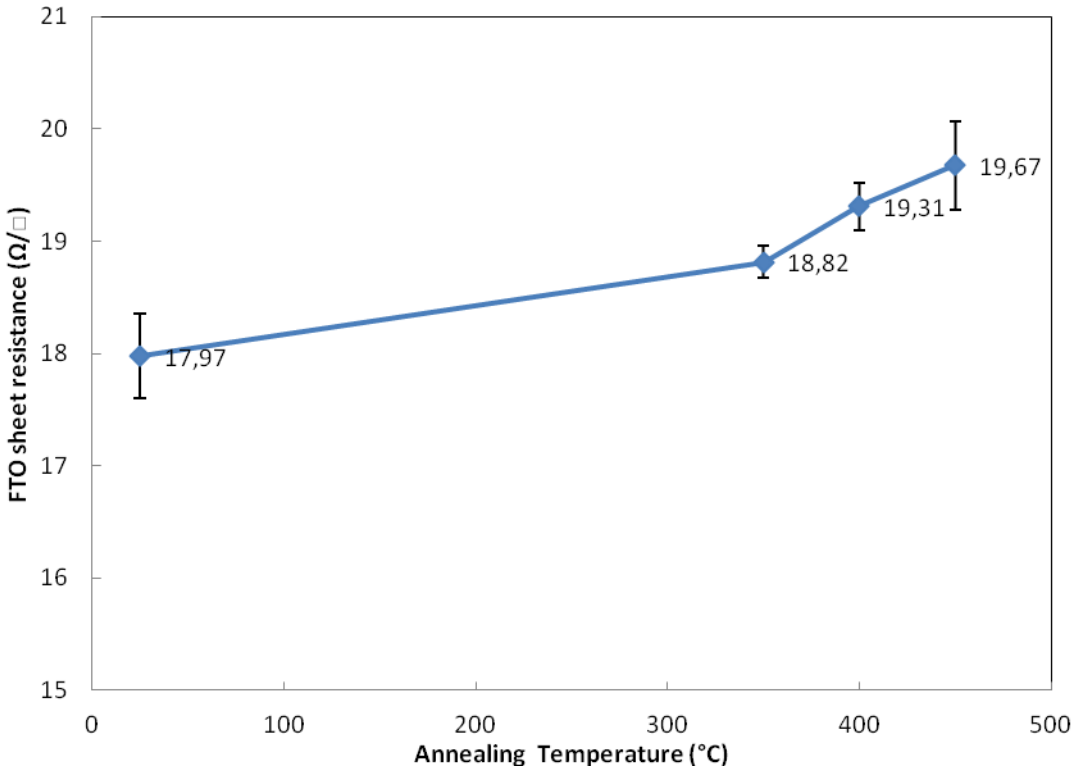

Figure S2. FTO sheet resistance variation after annealed at different temperature measured by four-point-probe technique.

Among the donor like defects, oxygen vacancy has the lowest formation energy. It has also been previously reported that the photoluminescence emission spectra from ZnO nanoparticles occurs due to the radiative energy loss of electrons from singly charged Zn interstitial and oxygen vacancies to the valence band confirming the existence of native impurity type in ZnO nanoparticles [25-27]. Therefore, impurities reduction upon annealing could lead to lower charge scattering or lower

resistance in ZnO layers as more perfect crystals are formed. While defect reduction in FTO could result in higher resistance, impurity reduction in ZnO film could enhance charge transfer through the film. To better understand the complex behavior of the charge transport process in DSSC, electrochemical impedance spectroscopy (EIS) was carried out.

The internal interface resistance can be regarded as the major obstacle for the charge transfer and charge collection in DSSCs, as these are composed of many interfaces; therefore, EIS is a suitable technique to investigate the interfacial electrical properties in this electrochemical cell. From EIS measurement, three semicircles for each annealing temperature were obtained in the Nyquist plot (Figure 4). The equivalent electrical model (inset of Figure 4) used to fit EIS data was then established based on the following assumptions. First, there are three main interfaces in a DSSC composing of the FTO/ZnO/dye/electrolyte, ZnO/dye/electrolyte and electrolyte/Pt/FTO, and these interfaces are represented by R_{ct2}, R_{ct1} and R_{ce} from low to high frequency, respectively. The first semicircle represents the resistance at the counter electrode-electrolyte interface (R_{ce}) corresponding to the high frequency region (100 mHz-30 kHz) as shown in Bode Plot (Figure 5). The second semicircle covers the intermediate frequency range representing the complex charge transfer behavior occurring at the photoelectrode, and is represented as R_{ct1} (100 mHz-3 kHz) and R_{ct2} (100 mHz-100 Hz). The third semicircle corresponding to the low frequency region (100 mHz-1 Hz) represents the Warburg diffusion behavior of electrolyte through inhomogeneous porous ZnO nanoparticles (porous Warburg impedance, Z_w, was used). The capacitance used in the model is regarded as double layer capacitance due to the porous surface of the photoelectrode [28]. Finally, the series resistance of the cell is presented by R_s and it is the parameter shifting the starting point of the semicircles.

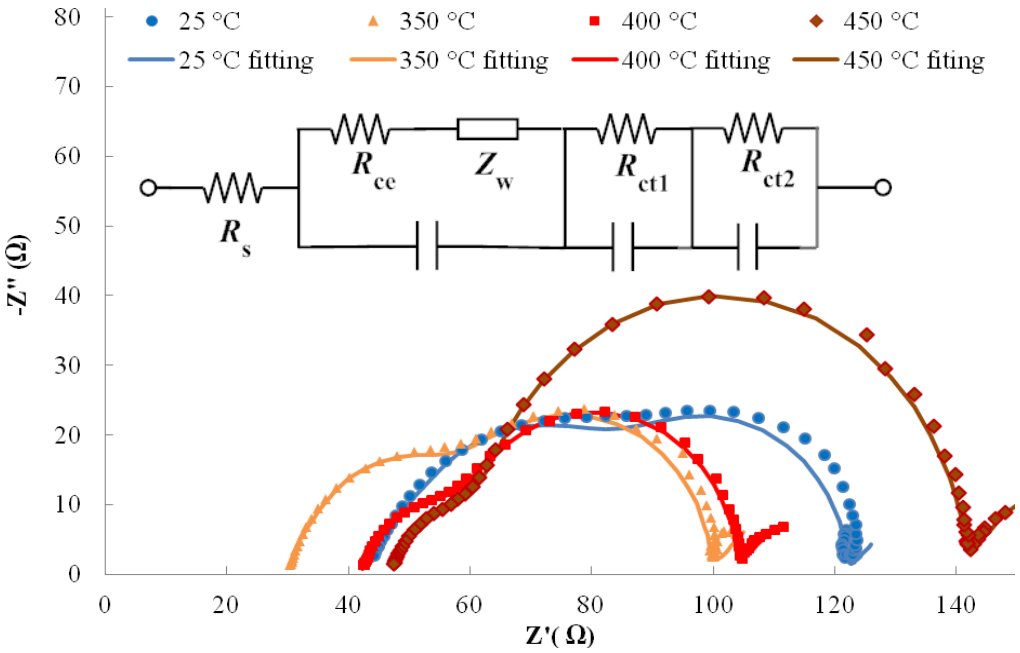

Figure 4. Nyquist plots of ZnO-DSSCs using photoelectrode annealed at different temperature (25°C, 350°C, 400°C and 450°C) with equivalent circuit model used in curve fitting.

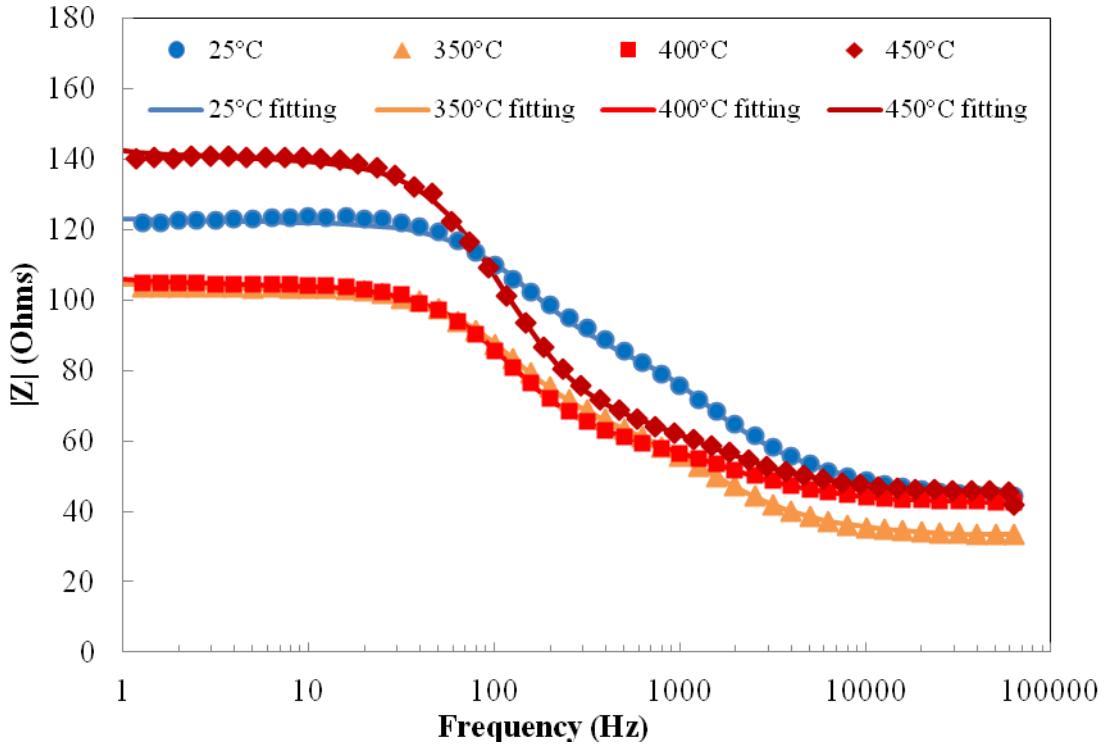

Figure 5. Bode plots of the ZnO DSSC using unannealed and annealed at 350°C, 400°C, and 450°Cphotoelectrodes, respectively.

The fitted results are shown in Table 1. The values of R_s and R_{ce} first decreases when ZnO photoelectrode was started to be annealed, and then increases with increase in annealing temperature. Relatively high resistances of unannealed sample (25°C) could be due to the poor electrical connection between FTO and ZnO film. The slight degradation of FTO substrate with annealing temperature causes the overall resistance to increase at higher annealing temperature.

Table 1. Parameters determined by fitting the EIS experimental data with equivalent circuit shown in Figure 3 inset.

EIS parameters	25°C	350°C	400°C	450°C
Rs (Ω)	43.73	37.81	42.05	45.26
Rce(Ω)	32.64	2.73	3.42	8.97
Rct1(Ω)	37.77	35.82	13.40	74.66
Rct2(Ω)	7.52	28.46	44.37	9.75
Zw(Ω)	6.85	10.57	11.09	15.00

It was found that the ZnO/dye/electrolyte interface resistance, R_{ct1}, reduces upon annealing and the lowest R_{ct1} was obtained at 400°C. This is expected to be due to better crystallinity of ZnO nanoparticles after thermal treatment. Since the interface for the generated charge to transfer and to recombine back to the dye or to electrolyte is the same, R_{ct1} can also be regarded as charge recombination resistance at the ZnO/dye/electrolyte interface. Therefore, it also infers that the highest charge recombination (mainly from ZnO to electrolyte) in this photoelectrode interface should be at 400°C. From current-voltage characteristic results (Figure 3), fill factor parameter shows the same trend as R_{ct1}. It is known that fill factor is a parameter relating to charge recombination in DSSC. Therefore the results from R_{ct1} and fill factor both confirm the highest electron recombination when the samples were annealed at 400°C. The collapsing of ZnO nanoparticle film was observed in this work which is similar to the work reported by Lu et.al.[13]. This causes new surface states which could act as electron trapping site resulted in abruptly increasing in R_{ct1} value at 450°C.

R_{ct2} represents the complex charge transfer behavior occurring at FTO/ZnO/dye/electrolyte interface. From Table 1, R_{ct2} increases upon annealing and reaches its highest value at 400°C. This indicates the difficulty in charge transfer through the interface at higher annealing temperature. On the other hand, the lowest charge recombination at the interface was also obtained when the photoelectrodes was annealed at 400°C. It is reported that electron recombination always occur either through the defects located on the semiconductor surface or by the recombination at the FTO and I_3^- in electrolyte interfaces [19].

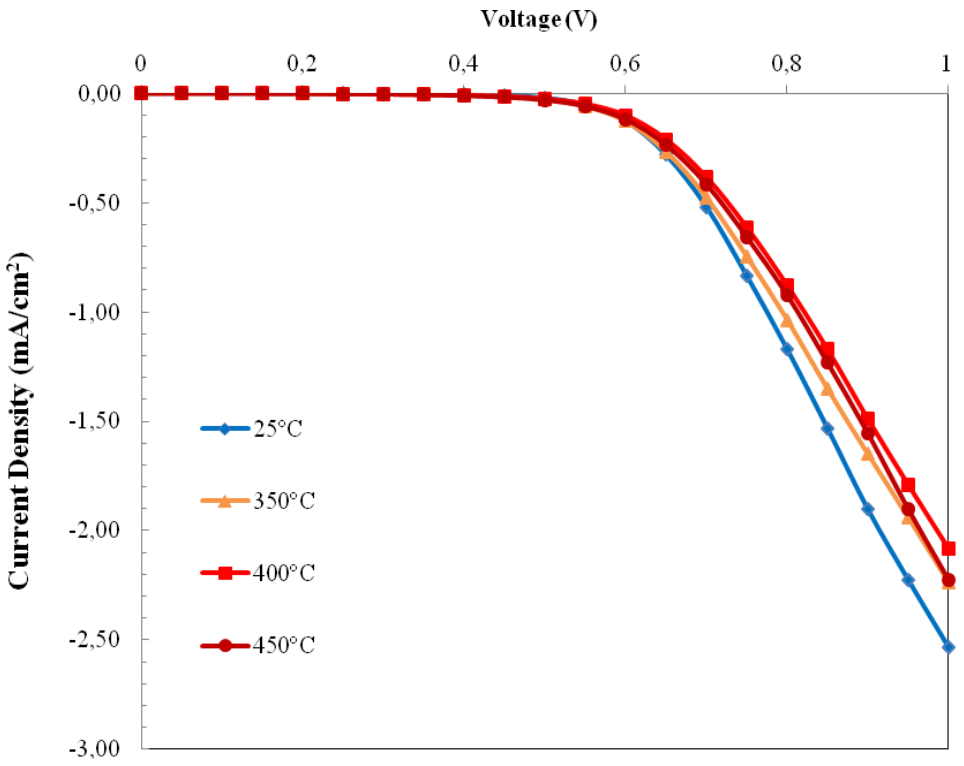

Figure 6. Current-voltage characteristics of ZnO-DSSC using different annealing temperature of photoelectrode measured under dark

However, the complex behavior in surface states due to the collapsing of ZnO nanoparticle at 450°C makes it difficult for this effect to be investigated. Nevertheless, it has been claimed that the dark current measurement could be used as a qualitative way to measure back electron transfer between the naked FTO site and tri-iodide ion through porous semiconductor [29]. The porous structure provides pathways for the liquid redox electrolyte to penetrate through the porous film and contact the bare conductive FTO surface. At these bare sites, the potential is thermodynamically favorable for the reduction of the oxidative species, mainly I_3^-. This causes electron recombination and results in the loss of photocurrent [29]. Therefore, the dark current measurement was performed to observe the effect of annealing on FTO/electrolyte recombination.

Figure 6 shows the dark current characteristics of ZnO nanoparticles DSSCs at different annealing temperatures from 25°C to 450°C. The dark current remains constant with the applied voltage until approximately 0.5 V. No significant change in the onset point with annealing temperature is seen. However, beyond 0.5 V, the current loss changes rapidly with voltage bias. It was found that, at the same bias voltage, increasing in annealing temperature suppresses charge loss up to 400°C. Further increasing in annealing temperature results in higher charge loss**.** This indicates the FTO/electrolyte recombination suppression upon annealing.

As described earlier, R_{ct2} represents FTO/ZnO/dye/electrolyte interface resistance, which relates to the ability of charge transfer through the interface. Therefore, the increase of R_{ct2} upon annealing up to 400°C agrees well with the lower charge recombination investigated by dark current measurement. Hence, it is possible to use R_{ct2} as an indicating parameter for back electron transfer between FTO and electrolyte. Using suitable EIS, electrical circuit model and current-voltage characterization with and without illumination, and the complex recombination in DSSC can be distinguished.

4. CONCLUSIONS

A compromise between charge generation and charge collection efficiency is the key to optimize ZnO-DSSC by thermal treatment. Annealing process affects the porosity and crystallinity of ZnO nanoparticle film. While the charge generation is suppressed by the lower surface area for dye loading, charge collection efficiency is enhanced through better charge transport channel with less charge recombination at FTO/ZnO/electrolyte interface. The optimized annealing temperature was obtained at 400°C. Further increasing the annealing temperature decreases cell efficiency as new surface defects are created by the collapse of ZnO porous structure.

ACKNOWLEDGEMENT

The authors would like to acknowledge the partial financial support from the Centre of Excellence in Nanotechnology and Energy Field of Study at Asian Institute of Technology, and the National Nanotechnology Center (NANOTEC) belonging to National Science & Technology Development Agency (NSTDA), Royal Thai Government. The authors also would like to thank the Physics Department of Khon Kaen University, Thailand for assisting with the EIS measurement.

References

1. H.A. Ribeiro, P.M. Sommeling, J.M. Kroon, A. Mendes and C.A.V. Costa, *Int. J. Green Energy*, 6 (2009) 245-256.
2. J. Yang, X. Liu, L. Yang, Y. Wang, Y. Zhang, J. Lang, M. Gao and B. Feng, *J. Alloys Comp.*, 477 (2009) 632-635.
3. M. Gratzel, *J. Photochem. Photobiology C: Photochemistry Reviews*, 4 (2003) 145-153.
4. M. Gratzel, *Acc. Chem. Res.*, 42 (2009) 1788-1798.
5. Q. Zhang and G. Cao, *Nano Today*, 6 (2011) 91-109.
6. Y. Chiba, A. Islam, Y. Watanabe, R. Komiya, N. Koide and L. Han, *Japanese J. Appl. Phys., Part 2: Letters*, 45 (2006) L638-L640.
7. B. Sunandan and D. Joydeep, *Sci. Technol. Adv. Mater.*, 10 (2009) 013001.
8. Q. Zhang, C.S. Dandeneau, X. Zhou and C. Cao, *Adv. Mater.*, 21 (2009) 4087-4108.
9. J. Park, H.J. Koo, B. Yoo, K. Yoo, K. Kim, W. Choi and N.G. Park, *Solar Energy Materials and Solar Cells*, 91 (2007) 1749-1754.
10. H. Tian, T. Yu and Z. Zou, *Mater. Sci.Forum*, 685 (2011) 13-19.
11. K.J. Chen, T.H. Fang, F.Y. Hung, L.W. Ji, S.J. Chang, S.J. Young and Y.J. Hsiao, *Appl. Surf. Sci.*, 254 (2008) 5791-5795.
12. H.H. Kyaw, T. Bora and J. Dutta, Zinc oxide nanorods Dye Sensitized Solar Cell: Effect of annealing temperature, 3rd Thailand Nanotechnology Conference 2009, Asian Institute of Technology, Thailand, 2009.
13. L. Lu, R. Li, K. Fan and T. Peng, *Solar Energy*, 84 (2010) 844-853.
14. J. Chung, J. Lee and S. Lim, *Physica B: Condensed Matter*, 405 (2010) 2593-2598.
15. C. Coskun, H. Guney, E. Gur and S. Tuzemen, *Turkish J. Phys.*, 33 (2009) 49-56.
16. N. Goswami and D.K. Sharma, *Physica E: Low-dimensional Systems and Nanostructures*, 42 (2010) 1675-1682.
17. M.C. Kao, H.Z. Chen and S.L. Young, *Applied Physics A: Materials Science and Processing*, 98 (2010) 595-599.
18. S. Sarkar, A. Makhal, T. Bora, S. Baruah, J. Dutta and S.K. Pal, *Phys. Chem. Chemical Phys.*, 13 (2011) 12488-12496.
19. Y. Zhang, L. Wu, Y. Liu and E. Xie, *J. Phys. D: Applied Physics*, 42 (2009).
20. S. Yang, Y. Liu, Y. Zhang and D. Mo, *Bull. Mater. Sci.*, 33 (2010) 209-214.
21. K. Park, Q. Zhang, B.B. Garcia and G. Cao, *J. Phys. Chem. C*, 115 (2011) 4927-4934.
22. P. Uthirakumar and C.-H. Hong, *Mater. Characterization*, 60 (2009) 1305-1310.
23. G.J. Exarhos and X.-D. Zhou, *Thin Solid Films*, 515 (2007) 7025-7052.
24. K. Ellmer and R. Mientus, *Thin Solid Films*, 516 (2008) 4620-4627.
25. M.A. Mahmood, S. Baruah and J. Dutta, *Mater. Chem. Phys.*, 130 (2011) 531-535.
26. J. Zhou, Y. Wang, F. Zhao, Y. Wang, Y. Zhang and L. Yang, *Journal of Luminescence*, 119-120 (2006) 248-252.
27. S. Baruah, S.S. Sinha, B. Ghosh, S.K. Pal, A.K. Raychaudhuri and J. Dutta, *Journal of Applied Physics*, 105 (2009).
28. S. Agarwala, L.N.S.A. Thummalakunta, C.A. Cook, C.K.N. Peh, A.S.W. Wong, L. Ke and G.W. Ho, *J. Power Sources*, 196 (2011) 1651-1656.
29. H. Yu, S. Zhang, H. Zhao, G. Will and P. Liu, *Electrochimica Acta*, 54 (2009) 1319-1324.